 doi:10.20944/preprints202205.0369.v1

Article

Carbamazepine Removal by Clay-Based Materials Using Adsorption and Photodegradation

Ilil Levakov[1], Yuval Shahar[1,2] and Giora Rytwo [1,2,*]

[1] Environmental Physical Chemistry Laboratory, MIGAL-Galilee Research Institute, Kiryat Shmona,1101602, Israel
[2] Environmental Sciences & Water Sciences Departments, Tel Hai College, Upper Galilee, 1220800 Israel
* Correspondence: rytwo@telhai.ac.il or giorarytwo@gmail.com; Tel.: +972-4-7700516

Abstract: Carbamazepine (CBZ) is one of the most common emerging contaminants released to the aquatic environment through domestic and pharmaceutical wastewater. Due to its high persistence through conventional degradation treatments, is considered a typical indicator for anthropogenic activities. This study tested the removal of CBZ through two different clay-based purification techniques: adsorption of relatively large concentrations (20-500 μmol L^{-1}) and photocatalysis of lower concentrations (<20 μmol L^{-1}). The sorption mechanism was examined by FTIR measurements, exchangeable cations released, and colloidal charge of the adsorbing clay materials. Photocatalysis was performed in batch experiments under various conditions. Despite the neutral charge of carbamazepine, the highest adsorption was observed on negatively charged montmorillonite-based clays. Desorption tests indicate that adsorbed CBZ is not released by washing. The adsorption/desorption processes were confirmed by ATR-FTIR analysis of the clay-CBZ particles. A combination of synthetic montmorillonite or hectorite with low H_2O_2 concentrations under UVC irradiation exhibits efficient homo-heterogeneous photodegradation at μM CBZ levels. The two techniques presented in this study suggest solutions for both industrial and municipal wastewater, possibly enabling water reuse.

Keywords: carbamazepine; adsorption; clay minerals; organoclays; advanced oxidation processes; photocatalysis; water reuse

1. Introduction

Carbamazepine (CBZ) is one of the most common emerging contaminants released into the aquatic environment through domestic and pharmaceutical wastewater[1]. It is mainly used for epilepsy and bipolar disorder treatments and is considered a typical indicator for anthropogenic activities due to its high persistence through degradation processes in regular wastewater treatments. The removal of carbamazepine during conventional wastewater treatment processes was found to be neglectable and didn't exceed 10% [1–3]. Therefore, carbamazepine is found worldwide in surface water, groundwater, soil, and even drinking water with various concentrations of up to 10 μg L^{-1} [4–7], and is expected to be found at higher levels in industrial wastewaters related to its manufacture and use (pharmaceutical and hospitals wastewater). Although no significant health risks were found associated with the exposure to carbamazepine residues in drinking water, several studies examined the negative side effect of consuming carbamazepine medicinally during pregnancy [8–10]. In addition, the ecotoxicity of carbamazepine for different aquatic species was demonstrated in many studies, revealing potential risks such as an increase in mortality rate, inhibition of growth, reproduction, and mobility [11–15]. The official regulations regarding carbamazepine in drinking water are limited and not available in most countries [7,16,17].

Over the years, various treatment approaches were tested aiming for efficient removal of carbamazepine from natural water bodies and wastewater. As mentioned above, removal by conventional technologies was found to be neglectable, but few advanced

 doi:10.20944/preprints202205.0369.v1

approaches were able to remove CBZ with relatively high efficiency. For example, integrating biological modification with activated sludge increased the removal rate [18–20], and specific microorganisms were found more efficient for its degradation [21,22]. In addition, advanced physicochemical treatment technologies such as nanofiltration (NF) and reverse osmosis (RO) were found to be effective for CBZ removal [23,24] even though the treatment of the concentrated brine afterward should be considered, and studies on that were not reported. Advanced oxidation processes [25,26] were an efficient option. Despite the high efficiency of those approaches, several problems limit their applicability, such as high costs, the toxicity of by-products in the oxidation process, biofouling, and the negative influence of natural organic matter during the removal by RO and NF [27–30].

Adsorption is one of the widest used approaches for CBZ removal. Activated carbon, is one of the common methods for adsorbing organic pollutants in drinking water, including pharmaceutically active compounds. The removal of carbamazepine by carbon-based sorbents was tested at various conditions with relatively high sorption capacities of up to 2 mmol g^{-1} [31–33]. Different clays and organoclay are also used as potential adsorbents for pharmaceutical pollution as a low-cost and effective technique. Adsorption of carbamazepine on various clays was examined in several studies. Adsorption studies on montmorillonite are inconclusive, while some studies present poor to low adsorption capacities (0-0.02 mmol g^{-1}) [34–37], others report considerably higher values (up to 0.15 mmol g^{-1}) [38,39]. Most studies have ascribed adsorption of CBZ on montmorillonite to Van der Waals interactions between the aromatic rings and the clay surface, and hydrogen bonds coordinating between oxygen atoms and exchangeable cations [35,37,39]. Khazri et al (2017) have demonstrated S-type isotherm, meaning low affinity at low concentration, but following initially adsorbed carbamazepine molecules, promotes subsequently increased adsorption by Van der Waals forces between the pollutant aromatic moitoes themselves. Some studies indicate that the adsorption occurred only on the clay's external surface and CBZ did not enter clays' interlayer space [35].

Photocatalysis, an advanced oxidation process (AOP), is an additional approach for removing carbamazepine from contaminated water bodies. While photolysis techniques without a catalyst provided relatively poor removal performances, the addition of a catalyst was found to improve the degradation rate significantly [7,30,40]. The most common heterogeneous photocatalysts for CBZ photodegradation are catalytic grade oxides such as TiO_2, ZnO, and MoS_2 [26,41,42]. The main disadvantages of using such conventional catalysts are the relatively high costs, difficulties with separation of the particles and their reuse, weak stability, and low quantum efficiency [43–45]. Therefore, modification and improvement of the bare catalysts are of high interest in water treatment research. In recent years, several studies demonstrate the applicability of using various clay-based materials as improved photocatalysts that provide efficient, low cost, and stable reactions [43,46–49]. Furthermore, irradiation of UVC light with a combination of a homogeneous catalyst as hydrogen-peroxide and clay-based heterogeneous catalysts may deliver an effective advanced oxidation process, as was recently shown for BPS [50]. Thus, low price, high adsorption capability, stable structure for regeneration, and distinctive spatial structure for possible modification may turn clay-based materials into optimal potential efficient photocatalysts.

This study reports the removal of carbamazepine through two different clay-based purification techniques, aiming for different purposes: adsorption of relatively large concentrations (up to 500 μmol L^{-1}), focusing on industrial effluents and brine from filtration devices, and photocatalysis of lower concentrations (<20 μmol L^{-1}), aiming complete removal in domestic wastewater. The first section of the article includes CBZ adsorption isotherms on natural or modified clay minerals (several smectites, sepiolite, and hydrophobically modified montmorillonite). Fit to Langmuir and dual-mode model [51,52] was evaluated, and interpretation of the sorption mechanism is presented based on measuring the cations released during the processes, FTIR, and colloidal particle charge of CBZ-clay. The second section includes photocatalysis of carbamazepine using UVC irradiation and combinations of homo- and heterogeneous synthetic clay catalysts. Comparison with P-

Preprints (www.preprints.org) | NOT PEER-REVIEWED | Posted: 27 May 2022 doi:10.20944/preprints202205.0369.v1

25® analogue TiO_2, which is considered a "gold standard" of heterogeneous catalysts [53,54] was performed. The main objective of the research was to suggest a solution for carbamazepine removal, a persistent emerging contaminant, in an effective, low-cost, and reliable manner, at both mM and μM concentrations, that might be applied to reuse both industrial and municipal wastewater.

2. Materials and Methods

2.1. Adsorption experiments

2.1.1. Materials

Clay minerals used for the adsorption study were S9 "Pangel" sepiolite purchased from Tolsa SA (Madrid, Spain), bentonite (commercial montmorillonite, CAS: 1302-78-9) from Sigma–Aldrich (Israel), and Ca- montmorillonite prepared from SWy-1 clay (purchased from the Source Clays Repository of The Clay Minerals Society) using a batch procedure [55]. Thiamine hydrochloride (B1, CAS: 67-03-8), benzalkonium (bzk) solution (50% in H_2O, CAS: 63449-41-2), and carbamazepine (CAS: 298-46-4) were supplied by Sigma–Aldrich (Israel).

2.1.2. Clay minerals modification and organoclay preparation

All clay and organoclay matrices were prepared according to the same procedure with a concentration of 1% (10 g clay L^{-1}). For the clay suspensions, 1 g of the relevant clay was gradually added to 100 ml of DDW while stirring with magnetic stirring until homogenous suspensions were obtained. For the organoclay suspensions, different organic cations were added to the homogeneous clay suspensions and the complex was agitated for 24 h in order to reach equilibrium. The bentonite-B1 organoclay (bent-B1) was prepared by the addition of 175g of thiamine powder to the bentonite suspension for a final load of 0.66 mmol thiamine g^{-1} of clay. The bentonite-bzk organoclay (bent-bzk) was prepared by adding 5.358 ml of benzalkonium solution (50%) for a total load of 0.6 mmol L^{-1}. Previous studies showed that at those loads there is no release of the adsorbed organocations. Adsorption of the organic modifier was estimated by mass balance, after measuring concentrations in the liquid phase. To ensure complete removal of non-strongly bound modifiers from the complexes, the suspensions were centrifuged (3000 rpm for 30 min) and 90% of the supernatant was replaced with DDW. This procedure was repeated three times. Concentrations of the modifiers in supernatants were below detection limits.

2.1.3. Adsorption isotherms

Several batch experiments were conducted to study the adsorption of carbamazepine on various clay-based matrices. Each experiment included a set of different carbamazepine concentrations added to the relevant clay or organoclay with three replicates for each concentration. The experiments were conducted in 50-ml plastic tubes with a constant amount of adsorbent, added concentrations of carbamazepine ranging from 0 to 0.45 mM (0-106 mg L^{-1}), and DDW added to a final volume of 50 ml. Details on concentrations of carbamazepine and the relevant matrices in each experiment are described in Table 1. After the addition of carbamazepine, the samples were kept at room temperature (23 ±1 C◦) on an orbital shaker (100 rpm) for 24 h to reach equilibrium. The equilibrium was confirmed by additional sampling and analysis after 48 h. To separate the solids from the supernatant, 2 ml from each tube were sampled to Eppendorf vials and centrifuged at 15,000 rpm for 25 min in a SciLogex D2012 Eppendorfs centrifuge. The concentration of carbamazepine and thiamine (in bent-B1 clay) were measured in the liquid phase using a diode-array HP 8452A UV–Vis spectrophotometer (Hewlett-Packard Company, Palo Alto, California, USA) and determined by optical density at 286 nm and 237 nm respectively. As a preliminary experiment, CBZ spectrum was measured under different pH values and found stable through the range of 1.3-13 (results not shown). The adsorbed amount of CBZ was estimated by mass balance, thus, subtracting the remaining concentration in the supernatant from the initial addition of carbamazepine. Average and

Preprints (www.preprints.org) | NOT PEER-REVIEWED | Posted: 27 May 2022 doi:10.20944/preprints202205.0369.v1

standard deviation values were calculated from the triplicates, for the measured concentration in equilibrium (X-axis in the isotherm) and the adsorbed CBZ (Y-axis in the isotherm).

Table 1. Detailed adsorption experiments' conditions.

Adsorbent type	Adsorbent concentration (g L^{-1})	Carbamazepine addition	
		(mmol g^{-1})	(mM)
Bentonite	0.25-0.4	0-2.0	0-0.43
Sepiolite	1.0	0-0.44	0-0.44
Ca- montmorillonite	0.3-0.4	0-1.5	0-0.45
Bentonite-B1 organoclay	0.5-0.6	0-1.0	0-0.47
Bentonite-benzalkonium organoclay	1	0-0.44	0-0.44

2.1.4. FTIR analysis

All sample suspensions were lyophilized (Christ Alpha 1-2 LD Plus, Germany) and the solids were analyzed in an attenuated total reflectance- Fourier transforms infrared (ATR-FTIR) spectrophotometer. Analysis was performed on a Nicolet iS10 FTIR (Nicolet Analytical Instruments, Madison, WI), using a SMART ATR device with a diamond crystal plate (Thermo Fisher Scientific, Madison, WI) within a range of wavenumbers of 4000 to 500 cm^{-1}. Spectra were recorded at 4 cm^{-1} nominal resolution with mathematical corrections yielding a 1.0 cm^{-1}actual resolution and averaged value from 50 measurements. The absorption intensity at different wavenumbers along the spectrum was quantified using TQ analyst EZ 8.0.2.97 software (Thermo Fisher Scientific Inc.). Quantification of adsorbed carbamazepine was based on the ratio between the absorbance intensities of specific absorption bands describing the sorbent in the case and CBZ [56]. In order to assess the stability of the CBZ adsorption, a release test was conducted subsequently to the adsorption experiments. The test was performed on three concentrations along the adsorption isotherms of CBZ to bentonite, Ca-SWy1, and bent-B1. After the adsorption experiment, the samples were washed for three cycles, including centrifugation (3000 rpm for 30 min) and replacement of 90% of the supernatant with distilled water. The washed samples were lyophilized, and the solids were analyzed again in the ATR-FTIR spectrophotometer.

2.1.5. Particle charge density measurements

The colloidal charge of the particles was measured using a particle charge detector (PCD) (BTG Mütek, PCD-05). The PCD was connected to an automatic titration unit (PCD-05 Travel Titrator) with polyelectrolytes. The particle charge measurement is based on electrodes measuring the colloidal charge of a suspension agitated mechanically by a piston, in combination with titration of a charge-compensating polyelectrolyte [57,58]. Poly-DADMAC (Poly-Diallyl-dimethyl-ammonium chloride) or PES-NA (Sodium-Polyethylensulfonate) were used as cationic and anionic polyelectrolytes according to the charge of the particles. Each measurement required 10 ml of the homogeneous suspension and colloidal charge results were normalized according to the mass of clay or organoclay in each case.

2.1.6. Exchangeable cations measurements

Examination of possible cations' exchange on the clay interlayers was evaluated by measuring the changes in cations concentrations in each of the supernatants of the adsorption points along the isotherm. Several major cations (calcium, sodium, potassium, and magnesium) were measured by inductively coupled plasma-optical emission spectrometry (ICP-OES) analysis. The analysis was performed with a Thermo Scientific IRIS Intrepid

Preprints (www.preprints.org) | NOT PEER-REVIEWED | Posted: 27 May 2022 doi:10.20944/preprints202205.0369.v1

II XDL ICP-OES (Thermo Electron Corporation, Waltham, MA, USA). All samples were filtered (0.2 μm) and HNO_3 was added to a final concentration of 2%. Multielement standard solution (multi-3 for ICP, 49596 Sigma-Aldrich) was used for calcium, magnesium, potassium, and sodium calibration, which calibration curves of 1-10, 0.2-2, 0.1-1, and 0.5-5 mg L^{-1} respectively.

2.1.7. Adsorption models

The fit of all adsorption isotherms to the Langmuir adsorption equation (Eq.1)

$$Cs = \frac{S_{max} K_L C_L}{1 + K_L C_L} \quad (1)$$

was tested. Cs is the sorbed concentration (mmol g^{-1}), C_L is the solution concentration (mM), S_{max} defines the number of adsorption sites per mass of sorbent (mmol g^{-1}), and K_L is the Langmuir adsorption coefficient (mM^{-1}).

Initially, all isotherms were also tested by the Dual-mode model (DMM) (Eq.2) which combines the Langmuir equation and a linear equation to simulate the combination of a site-specific adsorption mechanism and partitioning mechanism occurring simultaneously [52,59]. Nevertheless, the linear equation component was found to be neglectable, therefore only results of the Langmuir model are reported. The non-linear curve fitting was performed using scipy.optimize.curve_fit functions in Python, calculating the specific model parameters (S_{max} and K_L) for each isotherm.

2.2. Photocatalysis experiments

2.2.1. Materials

Catalyst-grade industrial high-quality TiO_2 (Hombikat®) and a 30% (9.79 M) concentrated H_2O_2 solution were purchased from Merck\Sigma–Aldrich (Merck KGaA, Darmstadt, Germany). SYn-1 Barasym SSM-100 synthetic mica-montmorillonite was obtained from the Source Clays Repository of The Clay Minerals Society, whereas Laponite-RD was provided by BYK-Chemie GmbH (Germany).

2.2.2. Methods

Degradation of CBZ from a 21.2 μM (5 mg L^{-1}) solution was measured in batch experiments in 100-mL UV-C-transparent quartz glass (refractive Index n = 1.5048), 5.3-cm diameter beaker placed in a Rayonet RMR-600 mini photochemical chamber reactor (Southern New England Ultraviolet Company, Branford, CT, USA), as described in previous studies [60,61]. The photoreactor was equipped with eight RMR 2537A lamps (254 nm wavelength), each lamp emitting an average irradiance flux of 19 W m^{-2} at 254 nm, equivalent to an overall intensity of 152 W m^{-2}, as measured in the center of the chamber using a Black Comet SR spectrometer with an F400 UV–VIS–SR-calibrated fiber optic probe equipped with a CR2 cosine light receptor (StellarNet Inc., Tampa, FL, USA). The Black Comet SR spectrometer was also used to measure the spectrum of the solutions during experiments using a 20 mm pathlength DP400 dip probe cuvette (StellarNet Inc., Tampa, FL, USA) placed inside the beaker. The solutions were constantly mixed with an external stirrer (VELP Scientifica, Usmate Velate, Italy) rotating at 100 rpm. Spectra were measured using the SpectraWiz software (StellarNet Inc., Tampa, FL, USA) every 10-20 s for approximately 20-60 min (depending on the experiment). The measurement procedure led to >150–400 data points for each experiment. Data were transformed to comma-separated values (CSV) files, and absorption of the net absorption of CBZ at 286 nm (ε_{286} = 12,826 M^{-1} cm^{-1}) was evaluated and downloaded after correcting the baseline. To allow comparison between parameters in different reaction mechanisms, the "relative dimensionless concentration at time t" [$A_{(t)}$] was evaluated [62] as $C_t/C_0 = OD_t/OD_0$ (the ratio of actual to initial concentration, or actual to initial light absorbance); thus A_0=1. Analysis of the data was performed as described in Section 2.2.3.

Preprints (www.preprints.org) | NOT PEER-REVIEWED | Posted: 27 May 2022 doi:10.20944/preprints202205.0369.v1

HPLC Chromatography measurements were performed to confirm that quantification using UV-Visible measurements. For this purpose, samples were filtered with a 0.22 micron spinning top filter, transferred to appropriate test tubes, and measured with an Agilent 1260 HPLC (Agilent Technologies Inc., USA, California) with a PDA detector and an inverted phase column LiChroCART® Purospher STAR RP-18 (Merck), covered at the edge (4.6 mm*25 cm) with a pore size of 5 µm. The eluents used for the run were UPW (Ultra-Pure Water) at a concentration of 0.1% formic acid (A) and methanol at a concentration of 0.1% formic acid (B). The flow rate was set at 1,000 µL min^{-1}, the injection volume was 60 µL, and the measured wavelength was 286 nm. HPLC measurements indeed confirm (results not shown) that direct UV-Visible spectroscopy measurements are accurate and effective at the required concentrations range (0.1-5 mg L^{-1}, ~0.5-25 µM).

The experiments performed included homogenous photocatalysis of CBZ with different concentrations (0.5-2.5 mg L^{-1}, 14.7-73.5 µM) of H_2O_2, heterogeneous photocatalysis of CBZ with various concentrations (0.2-1 mg L^{-1}) of TiO_2, barasym or laponite, and combined hetero-homogeneous photocatalysis of CBZ with 0.5 or 2.0 mg L^{-1} H_2O_2 and heterogeneous catalysts (TiO_2, barasym, laponite) at 0.2 mg L^{-1}.

2.2.3. Analysis of the data

In order to compare the efficacy of the different photocatalysis processes, an evaluation of the pseudo order, the kinetic rate, and the half-life of each process was performed. Calculations were done using the procedure extensively described in previous studies [50,63]. Considering the rate of change in concentration follows Eq-2:

$$\upsilon = \frac{d[A]}{dt} = -k_a[A]^{n_a} \tag{2}$$

where υ is the reaction rate, k_a is the apparent rate coefficient, A is the concentration of the pollutant in case, and n_a is the apparent or "pseudo" reaction order [64], the concentration at time t can be calculated if the kinetic rate coefficient k_a and the pseudo-order n_a are known(as long as $n_a \neq 1$), using:

$$[A]_{(t)} = \left(\frac{1}{\frac{1}{[A_0]^{n_a-1}} + (n_a - 1)k_a t} \right)^{\frac{1}{n_a-1}} \tag{3}$$

"Half-life time" ($t_{1/2}$), defined by the time it takes for the concentration of a reactant to reach half of its initial value [64], are easy-to-compare parameters, even in cases where pseudo orders are completely different. Half-life times can be evaluated by solving mathematically Equations (2) and (3) to the case were $[A]_{(t)} = 0.5$, yielding for $n_a \neq 1$

$$t_{1/2} = \frac{2^{n_a-1} - 1}{(n_a - 1)k_a[A_0]^{n_a-1}} \tag{4}$$

It should be emphasized that except for "first-order" processes, half-life times strongly depends on the initial concentration, as seen in Eq.4. This should be considered when comparing the efficiency of processes, and the use of a constant initial concentration of pollutants is important.

Pseudo-orders and kinetic coefficient that exhibits the best fit to each of the treatments were found as described in previous studies by a "bootstrap" [65,66] procedure based on choosing five random sets of 20 values from the several hundreds of data points in each experiment, and fitting the optimal parameters using the Solver tool in Excel® software [63].

 doi:10.20944/preprints202205.0369.v1

3. Results and discussion

3.1. Adsorption isotherms

Adsorption isotherms of carbamazepine on the different sorbents are presented in Figure 1A. The adsorption was tested as described in subsection 2.1.3 on five clay-based adsorbents, including 3 raw clays: (bentonite, Ca- SWy1, and sepiolite), and 2 organoclays prepared as described in chapter 2.1.2 (bent-bzk and bent-B1). The adsorption isotherms were also described by the Langmuir adsorption model, and the parameters S_{max} and K_L were evaluated (Table 2). R^2 and RMSE values between the observed and the calculated adsorption results indicate a good fit with the Langmuir model (Table 2, $R^2 > 0.99$).

Adsorption of CBZ on sepiolite is negligible. This is not obvious, since several non-charged molecules and oils are adsorbed in large amounts on this clay [67,68]. As for the smectites, organoclay based on BZK exhibited the lowest adsorption, whereas raw bentonite and Ca-SWy-1 adsorb more than 0.5 mmol g^{-1}. Such effect is unusual since smectites usually have a low affinity to non-charged organic molecules. However, it should be emphasized that at low CBZ concentration adsorption to those clays is almost zero (see Figure 1B, which shows adsorption isotherms at low CBZ concentrations), yielding an "S-type isotherm" [69]. This indicates that the direct interaction between the clay surface and the pollutant is low, and only after obtaining some coverage of the clay surface, adsorption increase. A similar observation was made in previous studies [39]. On the other hand, bent-B1 maximum adsorption is lower (app. 0.25 mmol g^{-1}, see Figure 1A) but it is also very efficient at low concentrations (see Figure 1B). The affinity of carbamazepine to bent-B1 increased considerably as demonstrated also in a higher calculated K_L value, 16.9 compared to 2.89 mM^{-1} on raw bentonite (Table 2). Due to the neutral charge of carbamazepine, it is assumed that more effective adsorption will be observed on the neutral charge particles such as bent-B1 and bent-bzk organoclays. Yet, higher adsorption capacities were found for montmorillonite clays. Studies reporting adsorption of CBZ on clay minerals mention lower adsorption values as 0.02-0.2 mmol g^{-1} [34,35,38]. Few studies have evaluated the adsorption on modified and organo-clays with even lower adsorbed amounts, from 0-0.05 mmol g^{-1} [70–73].

Despite bent-B1advantage in adsorption at low concentration, some thiamine (B1) was released from the bent-B1 complex during the adsorption process. The concentration of the released B1 was very low (averagely 0.02mM) with relatively constant values through different adsorption concentrations. Moreover, thiamine is considered a non-hazardous component that can provide a safe use under high standard regulations [74]. However, such instability in the behavior of the sorbent should be taken into consideration. B1 release interfered with UV Visible measurements, and in order to overcome this problem a simple mathematical spectra separation was performed, based on two well-known spectrums of the components (B1 and carbamazepine) at known concentrations, and calculating the mix spectrum by superposition [75] using the 'Solver'® optimization tool of the Microsoft Excel computer program.

Preprints (www.preprints.org) | NOT PEER-REVIEWED | Posted: 27 May 2022 doi:10.20944/preprints202205.0369.v1

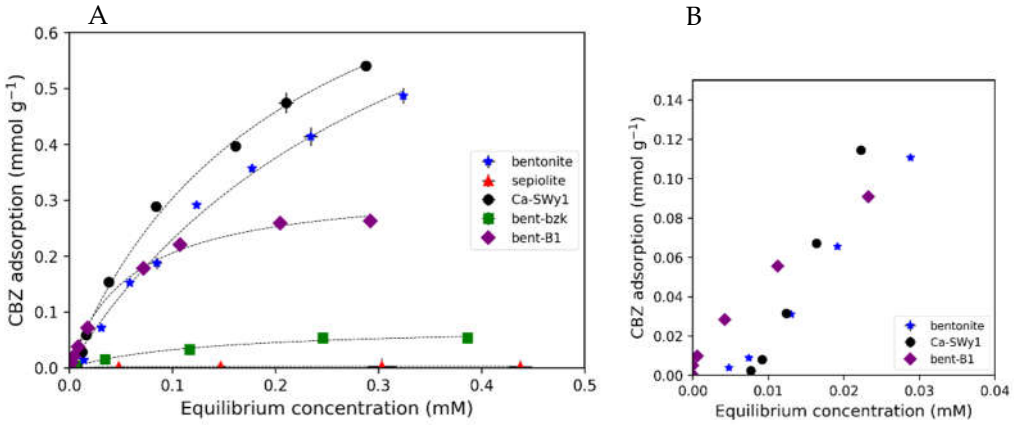

Figure 1. Adsorption isotherms of (A) carbamazepine on bentonite (blue asterisk), sepiolite (red triangle), Ca-SWy1 (black circle), bent-bzk (green square), and bent-B1 (purple diamond). Error bars represent triplicate standard deviations. The dashed lines represent Langmuir model predictions according to the estimated parameters detailed in Table 2. (B) Isotherms at low concentration of carbamazepine on bentonite, Ca-SWy1, and bent-B1.

Table 2. Langmuir model parameters for carbamazepine adsorption on clays and organoclays.

Adsorbent type	S_{max}(mmol g^{-1})	K_L(mM^{-1})	R^2	RMSE
Bentonite	1.02	2.89	0.993	0.014
Ca- SWy1	0.94	4.79	0.994	0.015
Bentonite-Benzalkonium organoclay	0.08	7.53	0.987	0.002
Bentonite- B1 organoclay	0.33	16.90	0.997	0.005

3.2. Colloidal charge

The influence of CBZ adsorption on the electrokinetic colloidal charge of bentonite, Ca- SWy1, and bent-B1 organoclay was evaluated (Figure 2) using a particle charge detector (PCD) as described in subsection 2.1.5. The initial colloidal charge of bentonite was significantly more negative than Ca-SWy1 due to the influence of the divalent calcium ions increasing neutralization on the Stern layer. Thus, in raw bentonite, the presence of monovalent sodium ions resulted in a more negative electrokinetic charge of the clay particles. The colloidal charge of the organoclay (bent-B1) was around zero due to the exchange of B1 with the inorganic ions, forming a non-charged surface. Similar values were observed in organoclays with organocations added at amounts near the cation exchange capacity of the clay as in B1-[51], berberine- [76], crystal violet, and tetraphenyl-phosphonium [77] smectites. For the raw bentonite and Ca-SWy-1, the increase in the electrokinetic colloidal charge, making it closer to neutralization, is attributed to the adsorption of the hydrophobic carbamazepine molecule. In raw bentonite, the increase in charge is accompanied by a cationic exchange of sodium with additional calcium arriving from the carbamazepine solution. Those results will be further discussed in the next chapters (3.3 and 3.4).

Preprints (www.preprints.org) | NOT PEER-REVIEWED | Posted: 27 May 2022 doi:10.20944/preprints202205.0369.v1

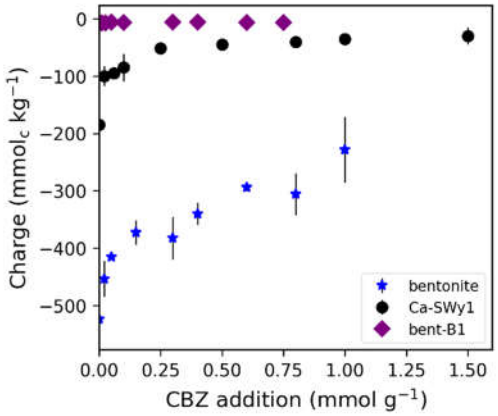

Figure 2. Colloidal charge of bentonite (blue asterisk), Ca-SWy1 (black circle), and bent-B1 organoclay (purple diamond) at different CBZ added amounts. .

3.3. Cation exchange in raw bentonite

The large adsorbed CBZ amounts on raw bentonite, led to the hypothesis that probably CBZ behaves as a cation, exchanging exchangeable cations from the raw clay. To test this hypothesis, ion exchange processes were examined as part of the adsorption mechanisms evaluation. Raw bentonite is reported to have a cation exchange capacity (CEC) of 0.8 mmole g^{-1}, whereas the cations composition is similar to the measured in SWy-1 and SWy-2 clays, thus- about 30% of the CEC is Na^+, while almost all the rest are divalent cations [55]. The release of inorganic cations due to the adsorption of CBZ was measured as described in subsection 2.1.6. It is interesting to mention that carbamazepine as purchased from Sigma contains some amounts of calcium in it. This was confirmed by measuring Ca concentrations in "pure" CBZ solutions, and reinforced by FTIR measurements reported in subsection 3.4 that exhibit a strong peak ascribed to $CaCO_3$. Figure 3A represents the release of sodium and calcium ions into the liquid phase as a function of the adsorption of carbamazepine. The release was calculated by subtracting the ions in the initial clay solution from the various solution concentrations after carbamazepine adsorption. The release of exchangeable sodium cations from the bentonite is linearly correlated to the amount of adsorbed carbamazepine (Figure 3A). Despite this linear correlation, CBZ adsorption is not completely explained by the sodium release and the ratio between carbamazepine adsorption and ion release was higher than 2. Thus, this is not a mere exchange CBZ/Na^+. Moreover, since calcium was added to the solution through the carbamazepine stock solution (as mentioned above), a comparison between the calcium addition and the release of sodium was conducted (Figure 3B), resulted in a linear correlation with a 1:1 ratio as for mmole$_c$. Thus, the hypothesis that CBZ exchanges Na^+ appears wrong, and a more reasonable explanation for the release of sodium cations is a Na^+/Ca^{2+} exchange process (Ca^{2+} coming from the CBZ solution), and the adsorption of carbamazepine did not include ions exchange on the clay's negative sites. To confirm this assumption, we performed the adsorption isotherms on Ca-SWy1, where all the CEC is *a-priori* saturated with Ca^{2+}. As shown in Figure 1A CBZ adsorption to Ca-SWy1 reaches similar and even slightly larger values than for raw bentonite, with similar Langmuir S_{max} values.

Preprints (www.preprints.org) | NOT PEER-REVIEWED | Posted: 27 May 2022 doi:10.20944/preprints202205.0369.v1

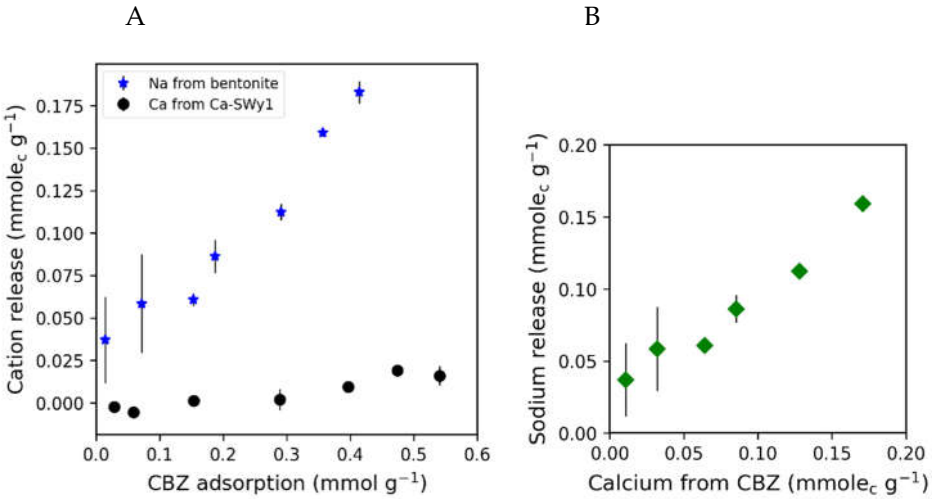

Figure 3. *(A)* Cations released to supernatant from bentonite (blue asterisk) or Ca-SWy1 (black circle) as a function of the adsorbed CBZ. (B) The addition of Ca^{+2} from CBZ solution (green diamonds).

3.4. FTIR analysis

One of the hypotheses to explain the relatively large adsorbed amounts of neutral CBZ on negatively charged clays was that as the matter of fact it undergoes degradation on the surface of the mineral, as was observed for example in the case of tri-methyl aryl dyes "adsorbed" on vermiculite VTx1 [78]. In order to test that, FTIR spectra of dried CBZ-clays were measured using an ATR device as described in subsection 2.1.4. The rationale aimed to confirm and evaluate the adsorption of carbamazepine on the absorbent particles by identifying the relevant structural group in the measured samples, whereas CBZ degradation will lead to different functional group vibrations. Figure 4A show the spectrum of CBZ, raw bentonite, and CBZ-bentonite at several carbamazepine amounts. CBZ-bentonite samples exhibit five absorption bands that were not observed in raw bentonite, at approximately 1640, 1570, 1490, and 1460-1435 cm^{-1}. Those absorption bands were correlated to typical peaks of functional groups of CBZ carbamazepine, as observed in the carbamazepine spectrum sample, and are known from the literature [79]. The only absorption band in raw bentonite in this region is at ~1630 cm^{-1} and ascribed to O-H deformation of hygroscopic water [80]. While the three CBZ absorption bands in the range 1400-1500 cm^{-1} (ascribed to C=C vibrations) are in almost the same place for adsorbed and raw CBZ, bands ascribed to C-N bond (at app. 1600 cm^{-1}) and to the amide group (NH_2 scissoring/C=O stretching, at ~1670 cm^{-1}) appear shifted to lower energies. This may indicate that the interaction between CBZ molecules and the clay is via the amide group.

An increase in all absorption bands in the range 1400-1700 cm^{-1} is observed accordingly to the adsorption process as measured in the experiment (Figure 4A). Relative quantification of the CBZ absorbed can be performed according to subsection 2.1.4, by calculating the ratio between the intensity or the area of CBZ absorption bands, to that of the structural O-H band related to the clay at 3620 cm^{-1}, where CBZ has no absorption at all. Subsequently, those ratios were compared to the amount of carbamazepine adsorbed to the clay as measured in the previous adsorption experiment (Figure 1). Figure 4C represents the comparison of two normalized absorption bands to the adsorption results, including the absorption bands' height at 1490 and their area at 1460-1435 cm^{-1}. The linear correlation (R^2>0.99) between the two data sets confirms the adsorption process as the reason for CBZ decrease in the equilibrium solution.

An additional absorption band was observed in the raw carbamazepine spectrum at approximately 1370 cm^{-1} and was not observed in any of the CBZ-bentonite samples (Figure 4A). According to the literature, these absorption bands may represent the presence of calcite ($CaCO_3$) in the carbamazepine source [80]. This is confirmed by a sharp absorption band at 870 cm^{-1} (results not shown) in the CBZ spectrum. The absence of this peak

Preprints (www.preprints.org) | NOT PEER-REVIEWED | Posted: 27 May 2022 doi:10.20944/preprints202205.0369.v1

in all CBZ-bentonite spectra indicates that calcite was released to the liquid phase, as correlated to the increase in calcium ions that was observed after adsorption (Figure 3). The stability of the CBZ adsorption was examined by a release test (as described in subsection 2.1.4). The results of the washed and original samples were compared, and no significant differences were observed in the absorption bands and the calculated ratios (results not shown). Hence, the adsorptions of CBZ to bentonite, Ca-SWy1, and bent-B1 were confirmed as stable processes without unexpected CBZ release.

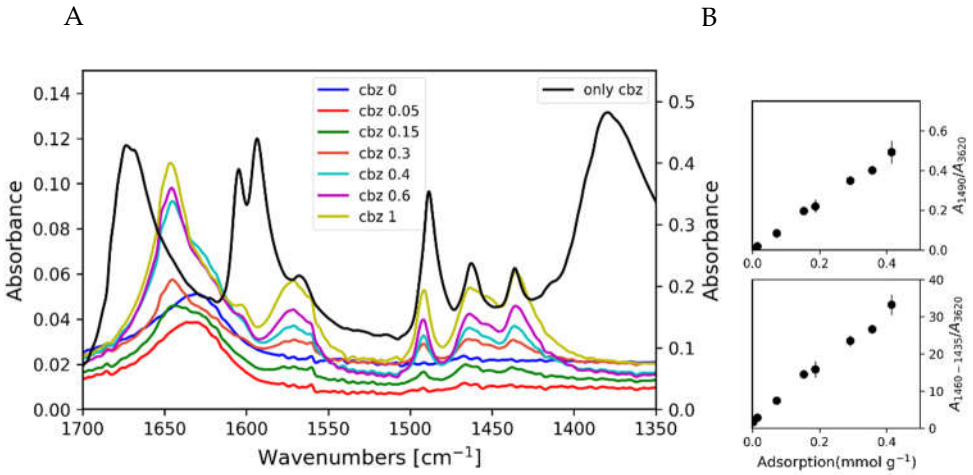

Figure 1. (A) ATR-FTIR spectra of CBZ (black, OD values on the right axis), bentonite raw clay (blue), and bentonite with added CBZ (in mmol g^{-1}) as denoted in the *legend (*OD values on the left axis). (B) normalized absorption bands height at 1490 and area at 1460-1435 cm^{-1} compared to the adsorption results as measured by the mass balance during the adsorption experiments.

3.5. Photocatalytic Degradation of Carbamazepine

3.5.1. Homogenous Photocatalysis with increasing concentrations of H_2O_2

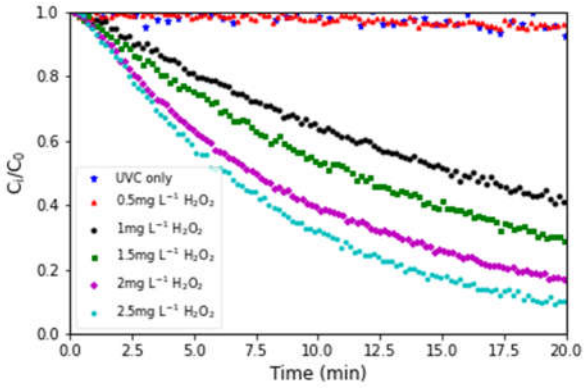

Figure 5. Photodegradation of 21.2 μM (5 mg L^{-1}) carbamazepine solution under UVC irradiation at several concentrations of hydrogen peroxide.

Figure 5 shows the photodegradation of a 21.2 μM (5 mg L^{-1}) CBZ solution, under UVC irradiation as described in subsection 2.2.2, with 0.5-2.5 mg L^{-1} (14.7-73.5 μM) H_2O_2 as homogenous catalysts. Such H_2O_2 concentration is in the range that was used recently for photodegradation of caffeine [60], but considerably lower than was usually used for photo- [81] or radio-catalysis [82] of CBZ. It can be seen that CBZ is stable under UVC radiation and doesn't undergo any photolysis. At the initial CBZ concentration used in this study (21.2 μM) very low H_2O_2 concentration (0.5 mg L^{-1}) exhibits almost no degradation, as in photolysis. Increasing the H_2O_2 concentrations to 1.0 mg L^{-1} changes the pseudo-

Preprints (www.preprints.org) | NOT PEER-REVIEWED | Posted: 27 May 2022 doi:10.20944/preprints202205.0369.v1

order as evaluated using Eq.2 and 3 from n=0 to n= 0.75, while $t_{1/2}$ as evaluated using Eq.4 changes from 219 to 15.6 min. Further increase of H_2O_2 to 2 or 2.5 mg L^{-1} reduces $t_{1/2}$ further to 7.6 and 6.4 min, respectively. Pseudo orders and half lifetimes of all experiments are shown also in Table 3.

Table 3. Pseudo-orders and half-life times for photodegradation experiments.

Heterogeneous catalyst		H_2O_2 (mg L^{-1})	Pseudo-Order n_a	Half-Life $t_{1/2}$ (min)
Type	(mg L^{-1})			
None	0	0	0	212.1 ± 1.56%
		0.5	0	219.3 ± 2.77%
		1.0	0.76 ± 4.31%	15.6 ± 0.62%
		1.5	0.93 ± 3.39%	11.4 ± 0.89%
		2.0	1.01 ± 2.65%	7.60 ± 1.00%
		2.5	0.82 ± 2.13%	6.39 ± 0.85%
TiO_2,	0.2	0	0	189.31 ± 2.53%
	0.4	0	0	122.2 ± 1.97%
	1	0	0	120.7 ± 2.66%
	0.2	0.5	0	68.0 ± 0.86%
	0.2	2.0	0.90 ± 3.10%	5.90 ± 1.39%
Barasym	0.2	0	0	296.7 ± 1.68%
	1.0	0	0	215.9 ± 1.74%
	0.2	0.5	1.24 ± 5.24%	33.2 ± 0.41%
	0.2	2.0	0.84 ± 1.99%	6.90 ± 0.92%
Laponite	0.2	0	No degradation	-
	1.0	0	No degradation	-
	0.2	0.5	1.04 ± 4.27%	37.0 ± 0.54%
	0.2	2.0	0.82 ± 3.27%	6.80 ± 1.03%

3.5.2. Heterogenous photocatalysis with TiO_2, barasym and laponite

Table 3 shows pseudo orders and half lifetime for the photodegradation of a 21.2 μM (5 mg/l) CBZ solution, under UVC irradiation, with 0-1 mg L^{-1} of commercial catalytic grade TiO_2 ("Degussa P25®" analogue), Barasym SSM-100 (synthetic montmorillonite) or Laponite® (synthetic hectorite) as heterogeneous catalysts. Synthetic clay minerals were chosen to avoid impurities present in natural minerals. P25® analogue TiO_2 was chosen as a "gold standard" since it is widely used for the photodegradation of organic refractory pollutants [83]. In most heterogeneous photocatalysis studies the catalyst concentration is from tens to thousands mg L^{-1} [84]. We chose to test relatively low concentrations of 0.2, 0.4 and 1 mg L^{-1} , based on our previous studies with BPS and ofloxacin [50,63]. It can be seen that the clay minerals have completely when added alone have almost no effect. TiO_2 indeed has some photocatalytic effect, but even at a 1 mg L^{-1} is not very effective ($t_{1/2}$ =121 min, n=0). Previous studies dealing with CBZ photodegradation used three orders of magnitude higher concentrations of TiO_2 as a heterogeneous catalyst and obtained half-life times of 10-20 minutes- considerably shorter than the present study [85,86].

3.5.3. Hetero-homogeneous photocatalysis

In previous studies [50,63] we have shown that a combination of low concentrations of both heterogeneous and homogeneous catalysts may yield synergistic effects, and speed up the photodegradation of priority pollutants such as BPS or ofloxacin. To test this effect on CBZ, we performed photodegradation experiments of a 21.2 μM (5 mg L^{-1}) CBZ solution, under UV irradiation, with a low concentration (0.2 mg L^{-1}) of the heterogeneous catalysts used in subsection 3.5.2, at two hydrogen peroxide levels: (a) high (2.0 mg L^{-1}) and (b) low (0.5 mg L^{-1}).

Preprints (www.preprints.org) | NOT PEER-REVIEWED | Posted: 27 May 2022 doi:10.20944/preprints202205.0369.v1

At 2 mg L^{-1} H_2O_2 concentration (results summarized in Table 3) the homogeneous catalyst already yields low $t_{1/2}$ values of less than 8 min. The addition of clays as heterogeneous catalysts makes almost no difference. As for TiO_2- it should be emphasized that when added alone at a low concentration (0.2 mg L^{-1}) almost no degradation is observed (Table 3), but the combination with 2.0 mg L^{-1} H_2O_2 slightly speeds up the process ($t_{1/2}$ changes from 6.4 to 5.9), and a small change in the pseudo- order is observed.

At a low homogeneous catalyst concentration of 0.5 mg L^{-1}, the influence of all heterogeneous catalysts is significant (Table 3): While with no heterogeneous catalyst $t_{1/2}$ at that hydrogen peroxide amount is about 219 min, the addition of 0.2 mg L^{-1} of TiO_2, barasym or laponite lowers $t_{1/2}$ to 68.0, 33.2 and 37.0 min, respectively. Pseudo-order also changes, especially for the clay minerals.

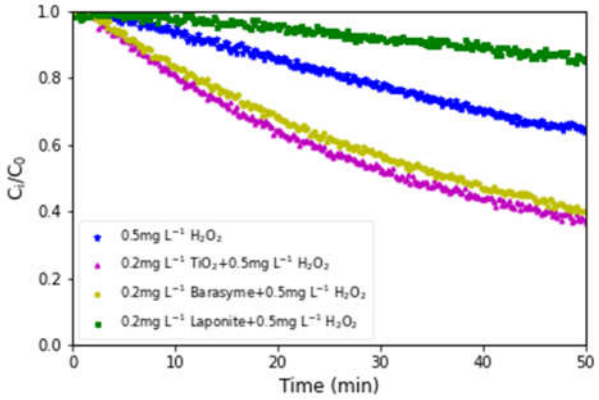

Figure 6. Photodegradation of a 21.2 μM (5 mg L^{-1}) carbamazepine under UVC irradiation, with 0.5 mg L^{-1} H_2O_2 alone or combined with 0.2 mg L^{-1} TiO_2, barasym or laponite.

4. Conclusions

CBZ removal at relatively large (>1 mM) concentrations in industrial effluents and nanofiltration brines, or at very low (<10 μM) concentrations should be removed in order to enable water reuse. Montmorillonite clays and organoclays may provide an efficient solution by adsorption for industrial effluents containing relatively high carbamazepine concentrations. Batch experiments have shown different adsorption capabilities of carbamazepine on various montmorillonite-based adsorbents, and in raw bentonite it might reach 0.5 mmole g^{-1}. The adsorption process was confirmed by ATR- FTIR analysis on the clay particles, and CBZ release was not observed, validating the stability of the sorbent-CBZ complexes. While B1-bentonite organoclay exhibits high affinity at low concentrations, an S-shape isotherm was observed for the raw clays, indicating low affinity at low adsorbed CBZ. However, the maximum capacity of raw montmorillonites is higher than for organoclay. In raw montmorillonites apparently, the initial coverage of the surface with CBZ molecules promotes enhanced adsorption of additional molecules probably by π-π interactions. According to the results, CBZ adsorption occurred only on clay surfaces, and the pollutant does not enter the internal pores of acicular clays as sepiolite. The high adsorption capability to the smectite raw clays on one hand and the low affinity at low concentrations, on the other hand, may provide a good solution for high concentrated contaminated solutions such as pharmaceutical wastewater or nano/microfiltration brine. Moreover, a combined implementation of raw montmorillonite clay and bent-B1 organoclay together can offer the advantages of raw clay for the high concentration and organoclay for the low carbamazepine concentrations.

As for AOP processes, it should be emphasized that since such processes are very specific- the description hereby focuses on the conditions of this study as for radiation intensity and CBZ concentrations. This study focuses on a relatively high initial concentration for municipal wastewater, even though there are several reports reaching such

levels [7,87]. Results indicate that direct photolysis with no additional catalyst does not yield CBZ degradation. The addition of hydrogen peroxide as homogeneous photocatalysts is very effective, but only above certain levels. (H_2O_2> 1 mg L^{-1}). The heterogeneous catalysts tested (including the "gold standard" P25 analogue TiO_2) at concentrations ranging 0-1 mg L^{-1} do not yield almost any CBZ degradation. Combined with high concentrations of H_2O_2 (2.0 mg L-1) effective degradation is observed, but this is mostly due to the homogeneous process. However, when combining a low amount of heterogeneous catalysts with very low H_2O_2 amounts (0.5 mg L-1) a synergistic effect is observed- and two treatments that each of them by itself are completely ineffective, lead to a relatively effective process. The advantage of low amounts of catalysts is obvious, considering the reuse of water will require the removal of the remains catalysts -both H_2O_2, and clays or TiO2.

The search for more effective water techniques is driving researchers toward AOPs. However, we should recall the limitations of AOPs in general and photocatalytic water treatment devices in particular: Since processes are very specific the challenge of dealing efficiently with multiple low-concentration priority pollutants, is far from being achieved. E.L. Cates [88]strongly criticizes the pursue for "new applications, improved catalysts, and reaction mechanisms", and summarizes that "it is time to stop patting ourselves on the back for laboratory “successes” that clearly turn a blind eye on fatal implementation hurdles". In this sense, probably a combination of processes such as adsorption on specifically tailored sorbents followed by advanced oxidation devices (or vice-versa) may yield more efficient and feasible water treatment technologies for both industrial and municipal wastewater.

Author Contributions: Conceptualization, G.R.; methodology, G.R., I.L & Y.S.; software, I.L & Y.S.; validation, G.R., I.L & Y.S.; formal analysis, G.R., I.L & Y.S.; investigation, G.R., I.L & Y.S.; resources, G.R.; data curation, I.L & Y.S.; writing—original draft preparation, G.R., I.L & Y.S.; writing—review and editing, I.L & G.R.; visualization, G.R., I.L & Y.S.; supervision, G.R.; project administration, G.R.; funding acquisition, G.R. All authors have read and agreed to the published version of the manuscript.

Funding: This research was partially funded by CSO-MOH (Israeli Ministry of Health), in the frame of the collaborative international consortium (REWA) financed under the 2020 AquaticPollutants Joint call of the AquaticPollutants ERA-NET Cofund (GA Nº 869178).

Acknowledgments: The authors would like to thank the European Commission and AKA (Finland), CSO-MOH (Israel), IFD (Denmark) and WRC (South Africa) for funding in the frame REWA international consortium (additional details in "funding" paragraph). REWA is an integral part of the activities developed by the Water, Oceans and AMR JPIs. The authors are also thankful to Mr. Chen Barak for all the technical support, Dr. Sara Azerrad for the HPLC support, and the whole team of the Hydrogeology and Examination of Soil Fertility Lab in MIGAL.

Conflicts of Interest: The authors declare no conflict of interest

References

1. Clara, M.; Strenn, B.; Kreuzinger, N. Carbamazepine as a possible anthropogenic marker in the aquatic environment: Investigations on the behaviour of Carbamazepine in wastewater treatment and during groundwater infiltration. *Water Res.* **2004**, *38*, 947–954.
2. Bahlmann, A.; Brack, W.; Schneider, R.J.; Krauss, M. Carbamazepine and its metabolites in wastewater: Analytical pitfalls and occurrence in Germany and Portugal. *Water Res.* **2014**, *57*, 104–114.
3. Ekpeghere, K.I.; Sim, W.J.; Lee, H.J.; Oh, J.E. Occurrence and distribution of carbamazepine, nicotine, estrogenic compounds, and their transformation products in wastewater from various treatment plants and the aquatic environment. *Sci. Total Environ.* **2018**, *640–641*, 1015–1023.
4. Bahlmann, A.; Carvalho, J.J.; Weller, M.G.; Panne, U.; Schneider, R.J. Immunoassays as high-throughput tools: Monitoring spatial and temporal variations of carbamazepine, caffeine and cetirizine in surface and wastewaters. *Chemosphere* **2012**, *89*, 1278–1286.
5. Dvory, N.Z.; Livshitz, Y.; Kuznetsov, M.; Adar, E.; Gasser, G.; Pankratov, I.; Lev, O.; Yakirevich, A. Caffeine vs. carbamazepine as indicators of wastewater pollution in a karst aquifer. *Hydrol. Earth Syst. Sci.* **2018**, *22*, 6371–6381.
6. Li, W.C. Occurrence, sources, and fate of pharmaceuticals in aquatic environment and soil. *Environ. Pollut.* **2014**, *187*, 193–201.

7. Hai, F.I.; Yang, S.; Asif, M.B.; Sencadas, V.; Shawkat, S.; Sanderson-Smith, M.; Gorman, J.; Xu, Z.Q.; Yamamoto, K. Carbamazepine as a Possible Anthropogenic Marker in Water: Occurrences, Toxicological Effects, Regulations and Removal by Wastewater Treatment Technologies. *Water (Switzerland)* **2018**, *10*, 1–32.
8. Cummings, C.; Stewart, M.; Stevenson, M.; Morrow, J.; Nelson, J. Neurodevelopment of children exposed in utero to lamotrigine, sodium valproate and carbamazepine. *Arch. Dis. Child.* **2011**, *96*, 643–647.
9. Jentink, J.; Dolk, H.; Loane, M.A.; Morris, J.K.; Wellesley, D.; Garne, E.; De Jong-van Den Berg, L. Intrauterine exposure to carbamazepine and specific congenital malformations: Systematic review and case-control study. *BMJ* **2010**, *341*, 1261.
10. Atkinson, D.E.; Brice-Bennett, S.; D'Souza, S.W. Antiepileptic medication during pregnancy: Does fetal genotype affect outcome? *Pediatr. Res.* **2007**, *62*, 120–127.
11. Hillis, D.G.; Antunes, P.; Sibley, P.K.; Klironomos, J.N.; Solomon, K.R. Structural responses of Daucus carota root-organ cultures and the arbuscular mycorrhizal fungus, Glomus intraradices, to 12 pharmaceuticals. *Chemosphere* **2008**, *73*, 344–352.
12. van den Brandhof, E.J.; Montforts, M. Fish embryo toxicity of carbamazepine, diclofenac and metoprolol. *Ecotoxicol. Environ. Saf.* **2010**, *73*, 1862–1866.
13. Han, G.H.; Hur, H.G.; Kim, S.D. Ecotoxicological risk of pharmaceuticals from wastewater treatment plants in Korea: Occurrence and toxicity to Daphnia magna. *Environ. Toxicol. Chem.* **2006**, *25*, 265–271.
14. Jos, A.; Repetto, G.; Rios, J.C.; Hazen, M.J.; Molero, M.L.; Del Peso, A.; Salguero, M.; Fernández-Freire, P.; Pérez-Martín, J.M.; Cameán, A. Ecotoxicological evaluation of carbamazepine using six different model systems with eighteen endpoints. *Toxicol. Vitr.* **2003**, *17*, 525–532.
15. Ferrari, B.; Paxéus, N.; Giudice, R. Lo; Pollio, A.; Garric, J. Ecotoxicological impact of pharmaceuticals found in treated wastewaters: Study of carbamazepine, clofibric acid, and diclofenac. *Ecotoxicol. Environ. Saf.* **2003**, *55*, 359–370.
16. Lofgren, H.; De Boer, R. Pharmaceuticals in Australia: Developments in regulation and governance. *Soc. Sci. Med.* **2004**, *58*, 2397–2407.
17. Vergili, I. Application of nanofiltration for the removal of carbamazepine, diclofenac and ibuprofen from drinking water sources. *J. Environ. Manage.* **2013**, *127*, 177–187.
18. Serrano, D.; Suárez, S.; Lema, J.M.; Omil, F. Removal of persistent pharmaceutical micropollutants from sewage by addition of PAC in a sequential membrane bioreactor. *Water Res.* **2011**, *45*, 5323–5333.
19. Li, X.; Hai, F.I.; Nghiem, L.D. Simultaneous activated carbon adsorption within a membrane bioreactor for an enhanced micropollutant removal. *Bioresour. Technol.* **2011**, *102*, 5319–5324.
20. Tiwari, B.; Sellamuthu, B.; Ouarda, Y.; Drogui, P.; Tyagi, R.D.; Buelna, G. Review on fate and mechanism of removal of pharmaceutical pollutants from wastewater using biological approach. *Bioresour. Technol.* **2017**, *224*, 1–12.
21. Marco-Urrea, E.; Pérez-Trujillo, M.; Vicent, T.; Caminal, G. Ability of white-rot fungi to remove selected pharmaceuticals and identification of degradation products of ibuprofen by Trametes versicolor. *Chemosphere* **2009**, *74*, 765–772.
22. Zhang, Y.; Geißen, S.U. Elimination of carbamazepine in a non-sterile fungal bioreactor. *Bioresour. Technol.* **2012**, *112*, 221–227.
23. Bellona, C.; Drewes, J.E.; Oelker, G.; Luna, J.; Filteau, G.; Amy, G. Comparing nanofiltration and reverse osmosis for drinking water augmentation. *J. Am. Water Works Assoc.* **2008**, *100*, 102–116.
24. Radjenović, J.; Petrović, M.; Ventura, F.; Barceló, D. Rejection of pharmaceuticals in nanofiltration and reverse osmosis membrane drinking water treatment. *Water Res.* **2008**, *42*, 3601–3610.
25. Li, Y.; Yang, Y.; Lei, J.; Liu, W.; Tong, M.; Liang, J. The degradation pathways of carbamazepine in advanced oxidation process: A mini review coupled with DFT calculation. *Sci. Total Environ.* **2021**, *779*, 146498.
26. Alharbi, S.K.; Price, W.E. Degradation and Fate of Pharmaceutically Active Contaminants by Advanced Oxidation Processes. *Curr. Pollut. Reports* **2017**, *3*, 268–280.
27. Simon, A.; Price, W.E.; Nghiem, L.D. Effects of chemical cleaning on the nanofiltration of pharmaceutically active compounds (PhACs). *Sep. Purif. Technol.* **2012**, *88*, 208–215.
28. Comerton, A.M.; Andrews, R.C.; Bagley, D.M. The influence of natural organic matter and cations on the rejection of endocrine disrupting and pharmaceutically active compounds by nanofiltration. *Water Res.* **2009**, *43*, 613–622.
29. Hajibabania, S.; Verliefde, A.; Drewes, J.E.; Nghiem, L.D.; McDonald, J.; Khan, S.; Le-Clech, P. Effect of fouling on removal of trace organic compounds by nanofiltration. *Drink. Water Eng. Sci.* **2011**, *4*, 71–82.
30. Alharbi, S.K.; Kang, J.; Nghiem, L.D.; van de Merwe, J.P.; Leusch, F.D.L.; Price, W.E. Photolysis and UV/H2O2 of diclofenac, sulfamethoxazole, carbamazepine, and trimethoprim: Identification of their major degradation products by ESI–LC–MS and assessment of the toxicity of reaction mixtures. *Process Saf. Environ. Prot.* **2017**, *112*, 222–234.
31. Décima, M.A.; Marzeddu, S.; Barchiesi, M.; Di Marcantonio, C.; Chiavola, A.; Boni, M.R. A review on the removal of carbamazepine from aqueous solution by using activated carbon and biochar. *Sustain.* **2021**, *13*.
32. Baghdadi, M.; Ghaffari, E.; Aminzadeh, B. Removal of carbamazepine from municipal wastewater effluent using optimally synthesized magnetic activated carbon: Adsorption and sedimentation kinetic studies. *J. Environ. Chem. Eng.* **2016**, *4*, 3309–3321.
33. To, M.H.; Hadi, P.; Hui, C.W.; Lin, C.S.K.; McKay, G. Mechanistic study of atenolol, acebutolol and carbamazepine adsorption on waste biomass derived activated carbon. *J. Mol. Liq.* **2017**, *241*, 386–398.
34. Alaghmand, M.; Alizadeh-Saei, J.; Barakat, S. Adsorption and removal of a selected emerging contaminant, carbamazepine, using Humic acid, Humasorb and Montmorillonite. Equilibrium isotherms, kinetics and effect of the water matrix. *J. Environ. Sci. Heal. - Part A Toxic/Hazardous Subst. Environ. Eng.* **2020**, *55*, 1534–1541.
35. Kryuchkova, M.; Batasheva, S.; Akhatova, F.; Babaev, V.; Buzyurova, D.; Vikulina, A.; Volodkin, D.; Fakhrullin, R.; Rozhina, E. Pharmaceuticals removal by adsorption with montmorillonite nanoclay. *Int. J. Mol. Sci.* **2021**, *22*.

36. Thiebault, T.; Boussafir, M.; Fougère, L.; Destandau, E.; Monnin, L.; Le Milbeau, C. Clay minerals for the removal of pharmaceuticals: Initial investigations of their adsorption properties in real wastewater effluents. *Environ. Nanotechnology, Monit. Manag.* **2019**, *12*.
37. Özçelik, G.; Bilgin, M.; Şahin, S. Carbamazepine sorption characteristics onto bentonite clay: Box-Behnken process design. *Sustain. Chem. Pharm.* **2020**, *18*.
38. Mahouachi, L.; Rastogi, T.; Palm, W.U.; Ghorbel-Abid, I.; Ben Hassen Chehimi, D.; Kümmerer, K. Natural clay as a sorbent to remove pharmaceutical micropollutants from wastewater. *Chemosphere* **2020**, *258*, 127213.
39. Khazri, H.; Ghorbel-Abid, I.; Kalfat, R.; Trabelsi-Ayadi, M. Removal of ibuprofen, naproxen and carbamazepine in aqueous solution onto natural clay: equilibrium, kinetics, and thermodynamic study. *Appl. Water Sci.* **2017**, *7*, 3031–3040.
40. Rytwo, G. Securing The Future: Clay-Based Solutions For a Comprehensive and Sustainable Potable-Water Supply System. *Clays Clay Miner.* **2018**, *66*, 315–328.
41. Haroune, L.; Salaun, M.; Ménard, A.; Legault, C.Y.; Bellenger, J.P. Photocatalytic degradation of carbamazepine and three derivatives using TiO2 and ZnO: Effect of pH, ionic strength, and natural organic matter. *Sci. Total Environ.* **2014**, *475*, 16–22.
42. Bo, L.; Liu, H.; Han, H. Photocatalytic degradation of trace carbamazepine in river water under solar irradiation. *J. Environ. Manage.* **2019**, *241*, 131–137.
43. Li, C.; Zhu, N.; Yang, S.; He, X.; Zheng, S.; Sun, Z.; Dionysiou, D.D. A review of clay based photocatalysts: Role of phyllosilicate mineral in interfacial assembly, microstructure control and performance regulation. *Chemosphere* **2021**, *273*, 129723.
44. Ong, C.B.; Ng, L.Y.; Mohammad, A.W. A review of ZnO nanoparticles as solar photocatalysts: Synthesis, mechanisms and applications. *Renew. Sustain. Energy Rev.* **2018**, *81*, 536–551.
45. Ning, F.; Shao, M.; Xu, S.; Fu, Y.; Zhang, R.; Wei, M.; Evans, D.G.; Duan, X. TiO 2 /graphene/NiFe-layered double hydroxide nanorod array photoanodes for efficient photoelectrochemical water splitting. *Energy Environ. Sci.* **2016**, *9*, 2633–2643.
46. Chong, M.N.; Jin, B.; Laera, G.; Saint, C.P. Evaluating the photodegradation of Carbamazepine in a sequential batch photoreactor system: Impacts of effluent organic matter and inorganic ions. *Chem. Eng. J.* **2011**, *174*, 595–602.
47. Vimonses, V.; Jin, B.; Chow, C.W.K.; Saint, C. An adsorption-photocatalysis hybrid process using multi-functional-nanoporous materials for wastewater reclamation. *Water Res.* **2010**, *44*, 5385–5397.
48. Zou, Y.; Hu, Y.; Shen, Z.; Yao, L.; Tang, D.; Zhang, S.; Wang, S.; Hu, B.; Zhao, G.; Wang, X. Application of aluminosilicate clay mineral-based composites in photocatalysis. *J. Environ. Sci. (China)* **2022**, *115*, 190–214.
49. Pérez-Carvajal, J.; Aranda, P.; Obregón, S.; Colón, G.; Ruiz-Hitzky, E. TiO2-clay based nanoarchitectures for enhanced photocatalytic hydrogen production. *Microporous Mesoporous Mater.* **2016**, *222*, 120–127.
50. Rytwo, G.; Levy, S.; Shahar, Y.; Lotan, I.; Zelkind, A.L.; Klein, T.; Barak, C. Health Protection Using Clay Minerals: A Case Study Based on the Removal of BPA and BPS from Water. *Clays Clay Miner.* **2021**, *69*, 641–653.
51. Ben Moshe, S.; Rytwo, G. Thiamine-based organoclay for phenol removal from water. *Appl. Clay Sci.* **2018**, *155*, 50–56.
52. Gonen, Y.; Rytwo, G. Using the dual-mode model to describe adsorption of organic pollutants onto an organoclay. *J. Colloid Interface Sci.* **2006**, *299*, 95–101.
53. Ohtani, B.; Prieto-Mahaney, O.O.; Li, D.; Abe, R. What is Degussa (Evonik) P25? Crystalline composition analysis, reconstruction from isolated pure particles and photocatalytic activity test. *J. Photochem. Photobiol. A Chem.* **2010**, *216*, 179–182.
54. Schneider, J.; Matsuoka, M.; Takeuchi, M.; Zhang, J.; Horiuchi, Y.; Anpo, M.; Bahnemann, D.W. Schneider et al. - 2014 - Understanding TiO 2 Photocatalysis Mechanisms and Materials(2).pdf. *Chem. Rev.* **2014**, *114*, 9919–9986.
55. Rytwo, G.; Serban, C.; Nir, S.; Margulies, L. Use of methylene blue and crystal violet for determination of exchangeable cations in montmorillonite. *Clays Clay Miner.* **1991**, *39*, 551–555.
56. Rytwo, G.; Zakai, R.; Wicklein, B. The Use of ATR-FTIR Spectroscopy for Quantification of Adsorbed Compounds. *J. Spectrosc.* **2015**, *2015*, 8 pp.
57. Dultz, S.; Rytwo, G. Effects of different organic cations on the electrokinetic surface charge from organo-montmorillonites - consequences for the adsorption properties. *"Clays Geotech. Econ. Interes. Swiss, Austrian Ger. Clay Gr. - DTTG Annu. Meet. Ger. Oct. 5th-8th, 2005, DTTG Reports* **2005**, *11*, 6–14.
58. Rytwo, G.; Chorsheed, L.L.; Avidan, L.; Lavi, R. Three Unusual Techniques for the Analysis of Surface Modification of Clays and Nanocomposites. In *Surface Modification of Clays and Nanocomposites*; Beall, G., Ed.; Clay Minerals Society: Boulder CO, 2016; Vol. 20, pp. 73–86 ISBN 9781881208457.
59. Vieth, W.R.; Sladek, K.J. A model for diffusion in a glassy polymer. *J. Colloid Sci.* **1965**, *20*, 1014–1033.
60. Rendel, P.; Rytwo, G. Degradation kinetics of caffeine in water by UV/H2O2 and UV/TiO2. *Desalin. Water Treat.* **2020**, *173*, 231–242.
61. Rendel, P.M.; Rytwo, G. The Effect of Electrolytes on the Photodegradation Kinetics of Caffeine. *Catalysts* **2020**, *10*, 644.
62. Rytwo, G.; Klein, T.; Margalit, S.; Mor, O.; Naftaly, A.; Daskal, G. A continuous-flow device for photocatalytic degradation and full mineralization of priority pollutants in water. *Desalin. Water Treat.* **2015**, *57*, 16424–16434.
63. Rytwo, G.; Zelkind, A.L. Evaluation of Kinetic Pseudo-Order in the Photocatalytic Degradation of Ofloxacin. *Catalysts* **2021**, *12*, 24.
64. Atkins, P.; de Paula, J. *Physical Chemistry*; W.H.Freemand and Co.: New York, 2006; Vol. 8th; ISBN 0-7167-8759-8.
65. Efron, B. Bootstrap Methods: Another Look at the Jackknife. *Ann. Stat.* **1979**, *7*, 1–26.
66. Mishra, D.K.; Dolan, K.D.; Yang, L. Bootstrap confidence intervals for the kinetic parameters of degradation of anthocyanins in grape pomace. *J. Food Process Eng.* **2011**, *34*, 1220–1233.

67. Zadaka-Amir, D.; Bleiman, N.; Mishael, Y.G. Sepiolite as an effective natural porous adsorbent for surface oil-spill. *Microporous Mesoporous Mater.* **2013**, *169*, 153–159.
68. Gutman, R.; Rauch, M.; Neuman, A.; Khamaisi, H.; Jonas-Levi, A.; Konovalova, Y.; Rytwo, G. Sepiolite Clay Attenuates the Development of Hypercholesterolemia and Obesity in Mice Fed a High-Fat High-Cholesterol Diet. *J. Med. Food* **2019**, jmf.2019.0030.
69. Sparks, D.L. *Environmental Soil Chemistry*; Academic Press, 1995; ISBN 9780126564457.
70. De Oliveira, T.; Boussafir, M.; Fougère, L.; Destandau, E.; Sugahara, Y.; Guégan, R. Use of a clay mineral and its nonionic and cationic organoclay derivatives for the removal of pharmaceuticals from rural wastewater effluents. *Chemosphere* **2020**, *259*.
71. Guégan, R.; De Oliveira, T.; Le Gleuher, J.; Sugahara, Y. Tuning down the environmental interests of organoclays for emerging pollutants: Pharmaceuticals in presence of electrolytes. *Chemosphere* **2020**, *239*.
72. Cabrera-Lafaurie, W.A.; Román, F.R.; Hernández-Maldonado, A.J. Transition metal modified and partially calcined inorganic-organic pillared clays for the adsorption of salicylic acid, clofibric acid, carbamazepine, and caffeine from water. *J. Colloid Interface Sci.* **2012**, *386*, 381–391.
73. Rivera-Jimenez, S.M.; Lehner, M.M.; Cabrera-Lafaurie, W.A.; Hernández-Maldonado, A.J. Removal of naproxen, salicylic acid, clofibric acid, and carbamazepine by water phase adsorption onto inorganic-organic-intercalated bentonites modified with transition metal cations. *Environ. Eng. Sci.* **2011**, *28*, 171–182.
74. Sunarić, S.; Pavlović, D.; Stanković, M.; Živković, J.; Arsić, I. Riboflavin and thiamine content in extracts of wild-grown plants for medicinal and cosmetic use. *Chem. Pap.* **2020**, *74*, 1729–1738.
75. Gonen, Y.; Rytwo, G. Using a Matlab Implemented Algorithm for UV-vis Spectral Resolution for pKa Determination and Multicomponent Analysis. *Anal. Chem. Insights* **2009**, *2009*, 21.
76. König, T.N.; Shulami, S.; Rytwo, G. Brine wastewater pretreatment using clay minerals and organoclays as flocculants. *Appl. Clay Sci.* **2012**, *67–68*, 119–124.
77. Rytwo, G.; Kohavi, Y.; Botnick, I.; Gonen, Y. Use of CV- and TPP-montmorillonite for the removal of priority pollutants from water. *Appl. Clay Sci.* **2007**, *36*, 182–190.
78. Rytwo, G.; Gonen, Y.; Huterer-Shveky, R. Evidence of degradation of triarylmethine dyes on Texas vermiculite. *Clays Clay Miner.* **2009**, *57*, 555–565.
79. Thilak Kumar, R.; Umamaheswari, S. FTIR, FTR and UV-Vis analysis of carbamazepine. *Res. J. Pharm. Biol. Chem. Sci.* **2011**, *2*, 685–693.
80. Madejová, J.; Komadel, P. Baseline studies of the clay minerals society source clays: infrared methods,. *Clays Clay Miner.* **2001**, *49*, 410–432.
81. Vogna, D.; Marotta, R.; Andreozzi, R.; Napolitano, A.; d'Ischia, M. Kinetic and chemical assessment of the UV/H2O2 treatment of antiepileptic drug carbamazepine. *Chemosphere* **2004**, *54*, 497–505.
82. Liu, N.; Lei, Z.-D.; Wang, T.; Wang, J.-J.; Zhang, X.-D.; Xu, G.; Tang, L. Radiolysis of carbamazepine aqueous solution using electron beam irradiation combining with hydrogen peroxide: Efficiency and mechanism. *Chem. Eng. J.* **2016**, *295*, 484–493.
83. Bouyarmane, H.; El Bekkali, C.; Labrag, J.; Es-saidi, I.; Bouhnik, O.; Abdelmoumen, H.; Laghzizil, A.; Nunzi, J.-M.; Robert, D. Photocatalytic degradation of emerging antibiotic pollutants in waters by TiO2/Hydroxyapatite nanocomposite materials. *Surfaces and Interfaces* **2021**, *24*, 101155.
84. Al-Mamun, M.R.; Kader, S.; Islam, M.S.; Khan, M.Z.H. Photocatalytic activity improvement and application of UV-TiO2 photocatalysis in textile wastewater treatment: A review. *J. Environ. Chem. Eng.* **2019**, *7*, 103248.
85. Carabin, A.; Drogui, P.; Robert, D. Photo-degradation of carbamazepine using TiO2 suspended photocatalysts. *J. Taiwan Inst. Chem. Eng.* **2015**, *54*, 109–117.
86. Im, J.-K.; Son, H.-S.; Kang, Y.-M.; Zoh, K.-D. Carbamazepine Degradation by Photolysis and Titanium Dioxide Photocatalysis. *Water Environ. Res.* **2012**, *84*, 554–561.
87. Kostich, M.S.; Batt, A.L.; Lazorchak, J.M. Concentrations of Prioritized Pharmaceuticals in Effluents from 50 Large Wastewater Treatment Plants in the US and Implications for Risk Estimation | US EPA Available online: https://www.epa.gov/water-research/concentrations-prioritized-pharmaceuticals-effluents-50-large-wastewater-treatment (accessed on May 11, 2022).
88. Cates, E.L. Photocatalytic water treatment: So where are we going with this? *Environ. Sci. Technol.* **2017**, *51*, 757–758.